From the currency rate quotations onto strings and brane world scenarios

D. Horváth[1,*] and R. Pincak[1,†]

[1]*SORS Research a.s, 040 01 Kosice, Slovak Republic*

(Dated: January 20, 2013)

Abstract

In the paper, we study numerically the projections of the real exchange rate dynamics onto the string-like topology. Our approach is inspired by the contemporary movements in the string theory. The string map of data is defined here by the boundary conditions, characteristic length, real valued and the method of redistribution of information. As a practical matter, this map represents the detrending and data standardization procedure. We introduced maps onto 1-end-point and 2-end-point open strings that satisfy the Dirichlet and Neumann boundary conditions. The questions of the choice of extra-dimensions, symmetries, duality and ways to the partial compactification are discussed. Subsequently, we pass to higher dimensional and more complex objects. The 2D-Brane was suggested which incorporated bid-ask spreads. Polarization by the spread was considered which admitted analyzing arbitrage opportunities on the market where transaction costs are taken into account. The model of the rotating string which naturally yields calculation of angular momentum is suitable for tracking of several currency pairs. The systematic way which allows one suggest more structured maps suitable for a simultaneous study of several currency pairs was analyzed by means of the Gâteaux generalized differential calculus. The effect of the string and brane maps on test data was studied by comparing their mean statistical characteristics. The study revealed notable differences between topologies. We review the dependence on the characteristic string length, mean fluctuations and properties of the intra-string statistics. The study explores the coupling of the string amplitude and volatility.

PACS numbers: 11.25.Wx, 89.65.Gh, 89.90.+n

*Electronic address: horvath@sors.com

†Electronic address: pincak@sors.com

1. INTRODUCTION

We are currently in the process of transfer of modern physical ideas into the neighboring field called econophysics. The physical statistical view point has proved fruitful, namely, in the description of systems where many-body effects dominate. However, standard, accepted by physicists, bottom-up approaches are cumbersome or outright impossible to follow the behavior of the complex economic systems, where autonomous models encounter the intrinsic variability.

Digital economy is founded on data. In the paper, we suggest and analyze statistical properties of heuristics based on the currency rate data which are arranged to mimic the topology of the basic variants of the physical strings and branes. Our primary motivation comes from the actual physical concepts [1, 2]; however, our realization differs from the original attempts in various significant details. The second aspect of our method is that it enables a transformation into a format which is useful for an analysis of a partial trend or relative fluctuations on the time scale window of interest.

As with most science problems, the representation of data is the key to efficient and effective solutions. The underlying link between our approach and the string theory may be seen in the switching from a local to a non-local form of the data description. This line passes from the single price to the multivalued collection of prices from the temporal neighborhood which we term here the string map. As we will see later, an important role in our considerations is played by the distance measure of the string maps. The idea of exploring the relationship between more intuitive geometric methods and financial data is not new. The discipline called the geometric data analysis includes many diverse examples of the conceptual schemes and theories grounded on the geometric representation and properties of data. Among them we can emphasize the tree network topology that exhibits usefulness in the studies of the world-trade network [3] and other network structures of the market constructed by means of inter-asset correlations [4, 5]. The multivariate statistical method called *cluster analysis* deals with data mapping onto representative subsets called *clusters* [6]. Here we work on the concept that is based on projection data into higher dimensional vectors in the sense of the work [7, 8]. Also, arguments based on the metrics are consistent with our efforts but not too obvious points in common with the original objectives of the nonlinear analysis.

The string theory development over the past 25 years achieved a high degree of popularity among physicists [9]. The reason lies in its inherent ability to unify theories that come from diverse physical spheres. The prime instrument of the unification represents the concept of extra dimension. The side-product of theoretical efforts can be seen in the elimination of the ultraviolet divergences of Feynman diagrams. However, despite the considerable achievements, there is a lack of the experimental verification of the original string theory. In contrast, in the present work we exploit time-series which can build the family of the string motivated models of boundary-respecting maps. In a narrow sense, the purpose of the present data-driven study is to develop statistical techniques for the analysis of these objects.

The work is organized as follows: In sec.2, we specify the data selection and data pre-treatment. In sec.3, we introduce the notion of the string map of data time series. The symmetry of the maps is discussed in sec.4. To examine generality and specificity of these ideas, the calculations have been performed for several representative currencies and ask (buyer initiated) or bid (seller initiated) prices. In sec.5, we give a generalization for a higher dimensional case which encodes the ask-bid spread difference. In this section, we also discuss the problem of partial compactification (subsection 5 A). The statistical picture (in sections 6, 7 and 8) is of primary interest. The analysis of fluctuations measured in the middle of a string by means of the statistical moments is carried out in sec.(6 B). In sec.7, we focus on the statistics of intra-string degrees of freedom. The efforts are in particular justified by the analytical studies in subsections sec.7 A and sec.7 B. They includes a decomposition of internal string states into Fourier modes in sec.7 C. In sec.8, we will see how the arbitrage opportunities, including spread, may be characterized by means of the model of *polarized string*. In the same section, we briefly discuss a reformulation of the popular concept of the correlation sum in terms of the strings and branes. There are also indications of a synergy between the string amplitudes and volatility in sec.6 C. Efforts have been made to study inter-currency relations by means of the projections onto *rotating strings* (sec.9) and via a generalization of the derivative (sec.10).

2. DATA ANALYSIS

First of all we need to mention some facts about data streams we analyzed. We analyze tick by tick data of EUR/USD, GBP/USD, USD/JPY, USD/CAD, USD/CHF major currency pairs from the OANDA market maker. We focussed on the three month period within three selected periods of 2009 which capture moments of the financial crisis. The streams are collected in such a way that each stream begins with Monday. More precisely, we selected periods denoted as Aug-Sep (from August 3rd. to September 7th.), Sep-Oct (Sep.7-Oct.5) and Oct-Nov (Sep.5-Nov.2). At first, the data sample has been decimated - only each 10th tick was considered. This delimits results to the scales larger than 10 ticks. The mean time corresponding to the string length $l_{\rm s}$ in ticks is given by

$$T(l_{\rm s}) = \langle t(\tau + l_{\rm s}) - t(\tau) \rangle \simeq \frac{1}{\tau_{\rm up} - \tau_{\rm dn}} \sum_{\tau=\tau_{\rm dn}}^{\tau_{\rm up}} \left[t(\tau + l_{\rm s}) - t(\tau) \right]. \tag{1}$$

Data for study of rotating strings and angular moments (see sec.9) were preformatted in a different way. In this case, the currency information has been projected onto the grid of the regularly spaced 10 sec intervals.

3. ONE DIMENSIONAL MAPS

By applying standard methodologies of detrending one may suggest to convert original series of the quotations of the mean currency exchange rate $p(\tau)$ onto a series of returns defined by

$$\frac{p(\tau + h) - p(\tau)}{p(\tau + h)}, \tag{2}$$

where h denotes a tick lag between currency quotes $p(\tau)$ and $p(\tau + h)$, τ is the index of the quote. The mean $p(\tau) = (p_{\rm ask}(\tau) + p_{\rm bid}(\tau))/2$ is calculated from $p_{\rm ask}(\tau)$ and $p_{\rm bid}(\tau)$.

In the spirit of the string theory it would be better to start with the 1-end-point open string map

$$P^{(1)}(\tau, h) = \frac{p(\tau + h) - p(\tau)}{p(\tau + h)}, \qquad h \in < 0, l_{\rm s} > \tag{3}$$

where superscript (1) refers to the number of endpoints.

Later, we may use the notation $P\{p\}$ which emphasizes the functional dependence upon the currency exchange rate $\{p\}$. It should also be noted that the use of P highlights the

canonical formal correspondence between the *rate of return* and the internal *string momentum*.

Here the tick variable h may be interpreted as a variable which extends along the extra dimension limited by the string size $l_{\rm s}$. A natural consequence of the transform, Eq.(3), is the fulfilment of the boundary condition

$$P^{(1)}(\tau, 0) = 0\,, \tag{4}$$

which holds for any tick coordinate τ. Later on, we want to highlight effects of the rare events. For this purpose, we introduce a power-law q-deformed model

$$P_q^{(1)}(\tau, h) = f_q\left(\frac{p(\tau+h) - p(\tau)}{p(\tau+h)}\right)\,, \qquad h \in < 0, l_{\rm s} > \tag{5}$$

by means of the function

$$f_q(x) = {\rm sign}(x)\,|x|^q\,, \qquad q > 0\,. \tag{6}$$

The 1-end-point string has defined the origin, but it reflects the linear trend in $p(.)$ at the scale $l_{\rm s}$. Therefore, the 1-end-point string map $P_q^{(1)}(.)$ may be understood as a q-deformed generalization of the *currency returns*. The illustration of the 1-end-point model is given in Fig.(1). The corresponding statistical characteristics displayed in Fig.(2) have been obtained on the basis of a statistical analysis discussed in section 2.

Clearly, the situation with a long-term trend is partially corrected by fixing $P_q^{(2)}(\tau, h)$ at $h = l_{\rm s}$. The open string with two end points is introduced via the nonlinear map which combines information about trends of p at two sequential segments

$$P_q^{(2)}(\tau, h) = f_q\left(\left(\frac{p(\tau+h) - p(\tau)}{p(\tau+h)}\right)\left(\frac{p(\tau+l_{\rm s}) - p(\tau+h)}{p(\tau+l_{\rm s})}\right)\right)\,, \qquad h \in < 0, l_{\rm s} > \,. \tag{7}$$

The map is suggested to include boundary conditions of *Dirichlet type*

$$P_q^{(2)}(\tau, 0) = P_q(\tau, l_{\rm s}) = 0\,, \qquad \text{at all ticks } \tau\,. \tag{8}$$

In particular, the sign of $P_q^{(2)}(\tau, h)$ comprises information about the behavior differences of $p(.)$ at three quotes (τ, $\tau + h$, $\tau + l_{\rm s}$). The $P_q^{(2)}(\tau, h) < 0$ occurs for trends of the different sign, whereas $P_q^{(2)}(\tau, h) > 0$ indicates the match of the signs.

In addition to the variable $P_q^{(2)}(\tau, h)$ we introduced the conjugate variable $X_q^{(2)}(\tau)$ via the recurrent summation

$$X_q^{(2)}(\tau, h+1) = X_q^{(2)}(\tau, h) + P_q^{(2)}(\tau, h-1)\,[\,t(\tau+h) - t(\tau+h-1)\,] \tag{9}$$

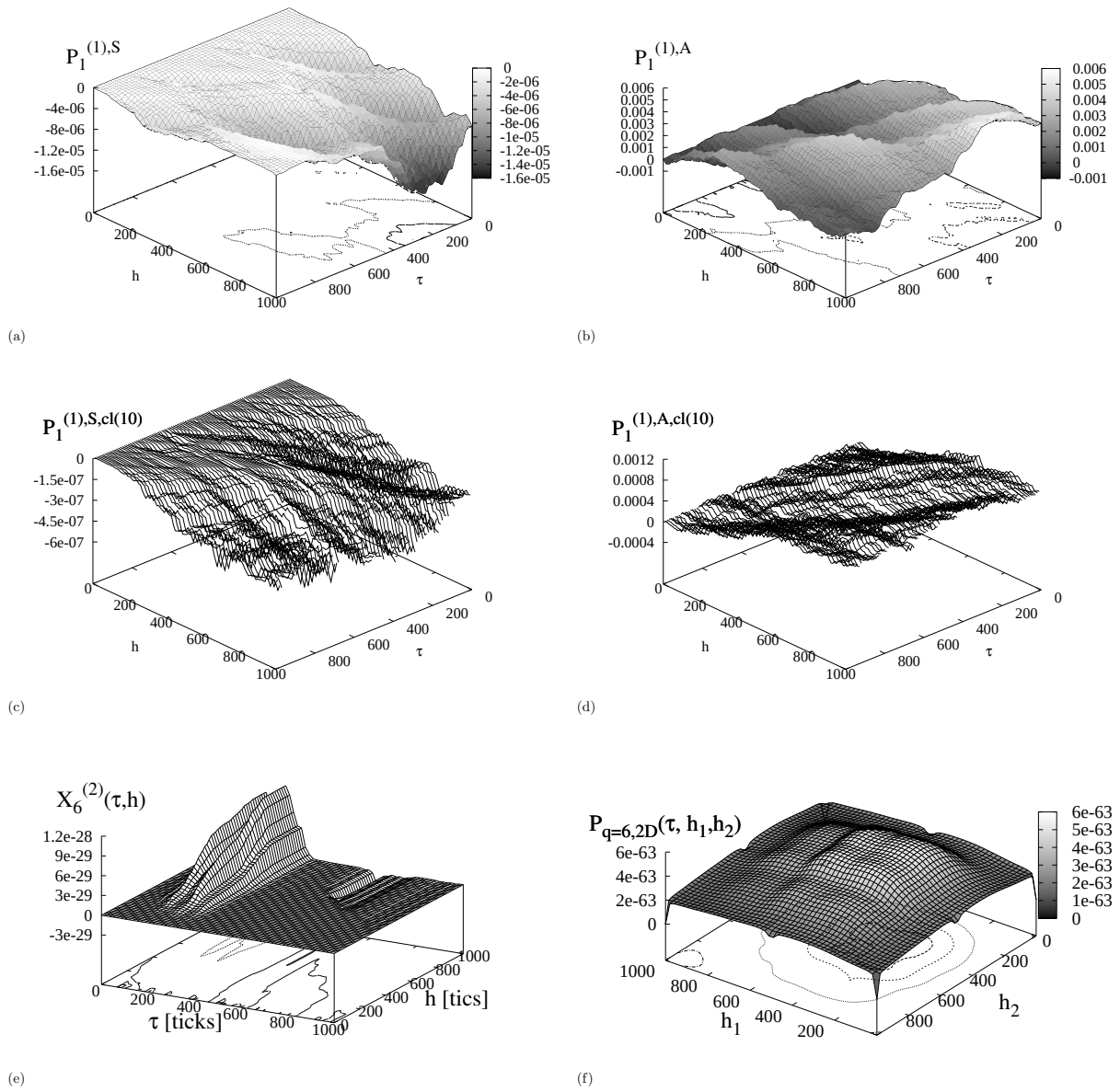

FIG. 1: The illustrative examples of the currency data map for GBP/USD. The parts (a)-(d) constructed for date Fri, 31 Jul 2009 time interval 15:06:37 - 15:43:09 GMT. Time evolution of symmetric ($P^{(1),\mathrm{S}}_{q=1}$) and anti-symmetric ($P^{(1),\mathrm{A}}$) component of the 1-end-point string of size $l_{\mathrm{s}} = 1000$ calculated for $q = 1$ (by means of Eq.(18)). In (c),(d) we see the same data mapped by means of the partially closed 1-end-point string ($q = 1$) for $N_{\mathrm{m}} = 10$, according to Eq.(26)). (e) The calculation carried out for the 2-end-point string for $l_{\mathrm{s}} = 1000$, $q = 6$ at some instant. We see that conjugate variable $X^{(2)}_{q=6}(\tau, h)$ satisfies the Neumann-type boundary conditions; (f) The instantaneous 2D-Brane state (date Fri, 31 Jul 2009 15:11:47 GMT) is computed according to Eq.(23).

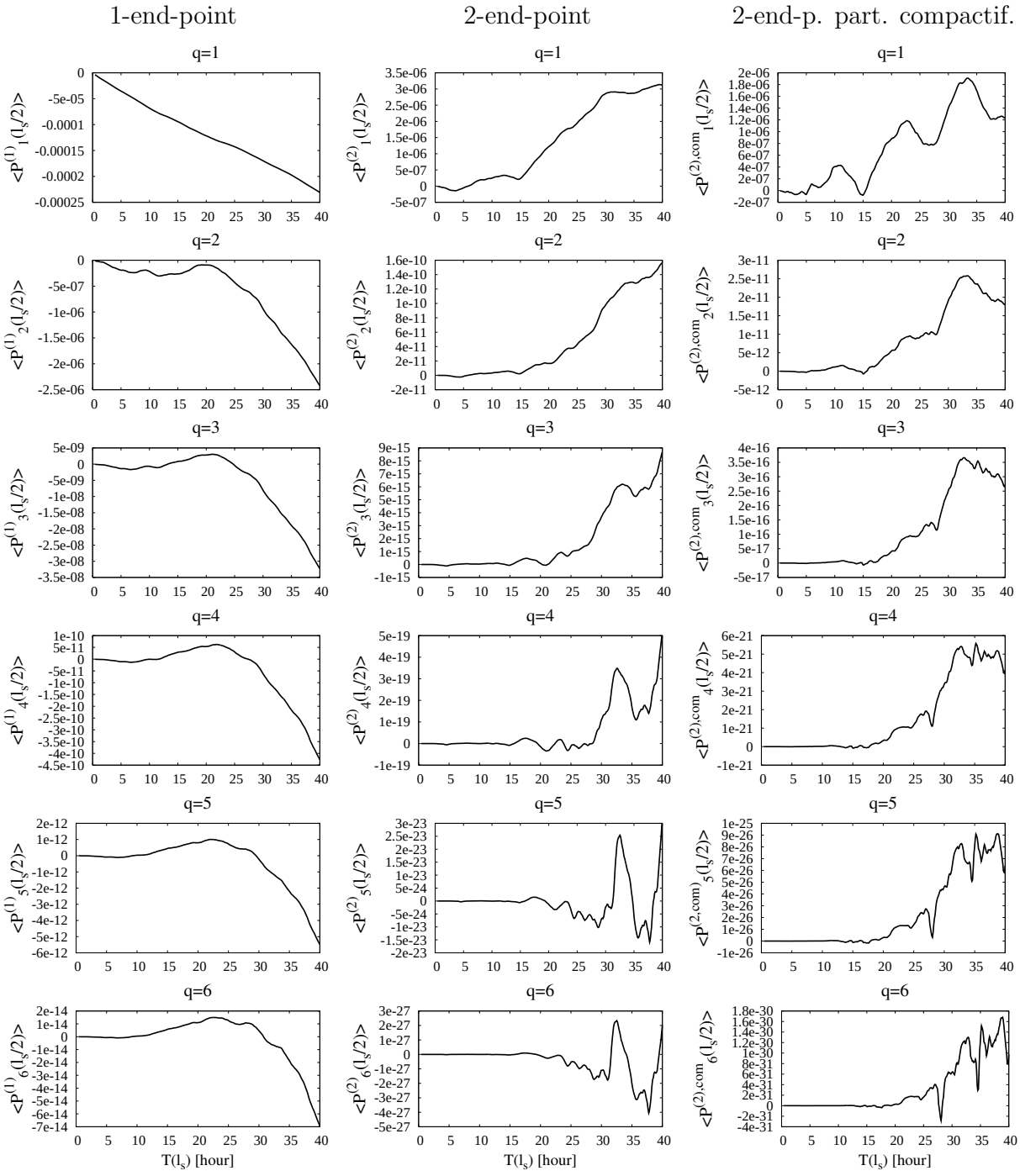

FIG. 2: The variability in statistical characteristics caused by differences in topology and q. Calculated for the period Aug-Sep, GBP/USD currency. The model with $q = 1$ has ability to reveal the currency long trend, on the other hand, the rare events are better visible for the 2-end-point string. The effect of the partial compactification with $N_{\rm m} = 4$ [see Eq.(26)] is demonstrated in the third column (again for the 2-end-point string).

(here $t(.)$ stands for a time-stamp corresponding to the quotation index τ in the argument). The above discrete form is suggested on the basis of the time-continuous Newton second law of motion $\dot{X}_q^{(2)}(t,h) = P_q^{(2)}(t,h)$ (written here for a unit mass). The form is equivalent to the imposing of the quadratic kinetic energy term $\frac{1}{2}(P_q^{(2)})^2$. Thus, the Hamiltonian picture [10] can be reconstructed in the following way;

$$\mathcal{H} = \frac{1}{2}\sum_{h=0}^{l_{\rm s}} \left[(\, P_q^{(2)}(\tau,h)\,)^2 - [\phi_{\rm ext}(\tau,h+1) - \phi_{\rm ext}(\tau,h)]\; X_q^{(2)}(\tau,h) \right] , \tag{10}$$

where $\phi_{\rm ext}(\tau,h)$ is the external field term which depends on the transform of the currency rate [see e.g. Eq.(7)]. We pass from the continuum to discrete theory by means of the functional form

$$\dot{P}_q^{(2)} \;=\; -\frac{\delta\mathcal{H}}{\delta X_q^{(2)}(h)} = \phi_{\rm ext}(\tau,h+1) - \phi_{\rm ext}(\tau,h) = P_q^{(2)}(\tau,h+1) - P_q^{(2)}(\tau,h)\,, \tag{11}$$

where $P_q^{(2)}(\tau,h)$ can be calibrated equal to $\phi_{\rm ext}(\tau,h)$.

The discrete conjugate variable meets the *Neumann type* boundary conditions

$$X_q^{(2)}(\tau,0) = X_q^{(2)}(\tau,1)\,, \qquad X_q^{(2)}(\tau,l_{\rm s}-1) = X_q^{(2)}(\tau,l_{\rm s})\,, \tag{12}$$

which is illustrated in Fig.(1)(d).

A more systematic way to obtain the 2-end-point string map represents the method of undetermined coefficients. The numerator of $q = 1$ can be chosen in the functional polynomial form of degree 2 with coefficients $\beta_0,\ldots,\beta_5$ as follows:

$$P_{q=1,{\rm Num}}^{(2)}(\tau,h) \;=\; \beta_0 p^2(\tau+h) + \beta_1 p^2(\tau) + \beta_2 p^2(\tau+l_{\rm s}) \tag{13}$$

$$+\; \beta_3 p(\tau)p(\tau+h) + \beta_4 p(\tau)p(\tau+l_{\rm s}) + \beta_5 p(\tau+h)p(\tau+l_{\rm s})\,. \tag{14}$$

Again, the Dirichlet conditions $P_{q=1,{\rm Num}}^{(2)}(\tau,0) = P_{q=1,{\rm Num}}(\tau,l_{\rm s}) = 0$ yield $P_{q=1,{\rm Num}}^{(2)} = \beta_0(p(\tau)-p(\tau+h))(p(\tau+l_{\rm s})-p(\tau+h))$ with arbitrary β_0. The overlooked denominator part of fraction $P_{q=1}^{(2)}$ then servers as a normalization factor.

Another interesting issue is the generalizing 1-end-point string to include the effect of many length scales

$$P_q^{(N_{l_{\rm s}})}(\tau,h;\{l\}) = \prod_{i=1}^{N_{l_{\rm s}}} f_q\left(\frac{p(\tau+l_i)-p(\tau+h)}{p(\tau+h)}\right) , \tag{15}$$

which relies on the sequence $\{l\} \equiv \{\, l_i,\; i = 1,\ldots,N_{l_{\rm s}}\}$, including the end points ($\min_{i=1,\ldots,N_{l_{\rm s}}} l_i$ and $\max_{i=1,\ldots,N_{l_{\rm s}}} l_i$) as well as the $N_{l_{\rm s}}-2$ interior node points that divide the string map into the sequence of unfixed segments of the non-uniform length (in general).

4. SYMMETRY WITH RESPECT TO $p(.) \to 1/p(.)$ TRANSFORM

The currency pairs can be separated into *direct* and *indirect* type. In a direct quote the *domestic* currency is the base currency, while the *foreign* currency is the quote currency. An *indirect* quote is just the opposite. Therefore, it would be interesting to take this symmetry into account. Hence, one can say that this two-fold division of the market network admits *duality symmetry*. Duality symmetries are some of the most interesting symmetries in physics. The term *duality* is used to refer to the relationship between two systems that have different descriptions but identical physics (identical trading operations).

Let us analyze the 1-end-point elementary string map when the currency changes from direct to indirect. The change can be formalized by means of the transformation

$$\hat{\mathcal{T}}_{\rm id} : P\{p(.)\} \to \overline{P}\{p(.)\} \equiv P\{1/p(.)\}\,, \tag{16}$$

For the 1-end-point map model of the string, Eq.(5), we obtained

$$\hat{\mathcal{T}}_{\rm id} P_q^{(1)}(\tau, h) = \overline{P}_q^{(1)}(\tau, h) = f_q\left(\frac{p(\tau) - p(\tau + h)}{p(\tau)}\right). \tag{17}$$

Let us consider two-member space of maps $V_P^{(1)} = \{P_q^{(1)}, \overline{P}_q^{(1)}\}$. Important, we see that $\hat{\mathcal{T}}_{\rm id}$ preserves the Dirichlet boundary conditions, in addition, the identity operator $\hat{\mathcal{T}}_{\rm id}^2$ leaves the elements of $V_P^{(1)}$ unchanged. The space $V_P^{(1)}$ is closed under the left action of $\hat{\mathcal{T}}_{\rm id}$. These ideas are straightforward transferable to the 2-end-point string points.

Now we omit the notation details and proceed according to Eq.(16). The map $P(.)$ is decomposable into a sum of symmetric and antisymmetric parts

$$P^{\rm S} = \frac{1}{2}(P + \overline{P})\,, \qquad P^{\rm A} = \frac{1}{2}(P - \overline{P}), \tag{18}$$

respectively. Due to of normalization by $1/2$, we get the projection properties

$$\hat{\mathcal{T}}_{\rm id} P^{\rm S} = P^{\rm S}\,, \qquad \hat{\mathcal{T}}_{\rm id} P^{\rm A} = -P^{\rm A}\,. \tag{19}$$

To be more concrete, we choose $q = 1$ and obtain

$$P_{q=1}^{(1),{\rm S}} = 1 - \frac{1}{2}\left[\frac{p(\tau)}{p(\tau + h)} + \frac{p(\tau + h)}{p(\tau)}\right], \qquad P_{q=1}^{(1),{\rm A}} = \frac{1}{2}\left[\frac{p(\tau)}{p(\tau + h)} - \frac{p(\tau + h)}{p(\tau)}\right]. \tag{20}$$

and

$$\begin{aligned} P_1^{(2),{\rm A}} &= \frac{1}{2}\left[\frac{p(\tau)}{p(\tau + l_{\rm s})} - \frac{p(\tau + l_{\rm s})}{p(\tau)} + \frac{p(\tau + h)}{p(\tau)} - \frac{p(\tau)}{p(\tau + h)} + \frac{p(\tau + l_{\rm s})}{p(\tau + h)} - \frac{p(\tau + h)}{p(\tau + l_{\rm s})}\right], \\ P_1^{(2),{\rm S}} &= 1 + \frac{1}{2}\left[\frac{p(\tau + l_{\rm s})}{p(\tau)} + \frac{p(\tau)}{p(\tau + l_{\rm s})} - \frac{p(\tau)}{p(\tau + h)} - \frac{p(\tau + h)}{p(\tau)} - \frac{p(\tau + h)}{p(\tau + l_{\rm s})} - \frac{p(\tau + l_{\rm s})}{p(\tau + h)}\right]. \end{aligned} \tag{21}$$

We see that the $P^{(1),\mathrm{S}}_{q=1}$ and $P^{(2),\mathrm{S}}_{q=1}$ maps acquire formal signs of the systems with $T-$*dual symmetry* [2]. When the world described by the closed string of the radius R is indistinguishable from the world of the radius $\propto 1/R$ for any R, the symmetry manifests itself by $(R \pm \mathrm{const.}/R)$ terms of the mass squared operator. The correspondence with our model becomes apparent one assumes that R corresponds to the ratio $p(\tau)/p(\tau+h)$ in Eq.(20). However, we must also refer a reader to an apparently serious difference that in our model we do not consider for the moment the compact dimension.

A. $\mathcal{T}_{\mathrm{id}}$ transform under the conditions of bid-ask spreads

Simply, the generalization can also be made with allowing for currency variables which appear as a consequence of the transaction costs [11]. The occurrence of ask-bid spread complicates the analysis in several ways. Instead of one price for each currency, the task requires the availability to two prices. The impact of ask-bid spread on the time-series properties has been studied within the elementary model [12].

Thus, for the purpose of a thorough and more realistic analysis of the market information, it seems straightforward to introduce generalized transform

$$\hat{\mathcal{T}}^{\mathrm{ab}}_{\mathrm{id}} P\{\, p_{\mathrm{ask}}(.), p_{\mathrm{bid}}(.)\,\} = \overline{P}\{\, 1/p_{\mathrm{bid}}(.), 1/p_{\mathrm{ask}}(.)\,\}\,, \tag{22}$$

which converts to Eq.(17) in the limit of vanishing spread.

5. MAPPING TO THE MODEL OF 2D BRANE

Clearly, there is a possibility to go beyond a string model towards more complex maps including alternative spread-adjusted currency returns. Formally, the generalized mapping onto the 2D brane with the $(h_1, h_2) \in < 0, l_{\mathrm{s}} > \times < 0, l_{\mathrm{s}} >$ coordinates which vary along two extra dimensions could be proposed in the following form:

$$\begin{aligned} P_{2\mathrm{D},q}(\tau, h_1, h_2) \;=\; & f_q \left(\left(\frac{p_{\mathrm{ask}}(\tau+h_1) - p_{\mathrm{ask}}(\tau)}{p_{\mathrm{ask}}(\tau+h_1)} \right) \left(\frac{p_{\mathrm{ask}}(\tau+l_{\mathrm{s}}) - p_{\mathrm{ask}}(\tau+h_1)}{p_{\mathrm{ask}}(\tau+l_{\mathrm{s}})} \right) \right. \\ & \times \left. \left(\frac{p_{\mathrm{bid}}(\tau) - p_{\mathrm{bid}}(\tau+h_2)}{p_{\mathrm{bid}}(\tau)} \right) \left(\frac{p_{\mathrm{bid}}(\tau+h_2) - p_{\mathrm{bid}}(\tau+l_{\mathrm{s}})}{p_{\mathrm{bid}}(\tau+h_2)} \right) \right) . \end{aligned} \tag{23}$$

The map constituted by the combination of "bid" and "ask" quotes is constructed to satisfy the Dirichlet boundary conditions

$$P_{2\mathrm{D},q}(\tau, h_1, 0) = P_{2\mathrm{D},q}(\tau, h_1, l_\mathrm{s}) = P_{2\mathrm{D},q}(\tau, 0, h_2) = P_{2\mathrm{D},q}(\tau, l_\mathrm{s}, h_2)\,. \tag{24}$$

In addition, the above construction, Eq.(23), has been chosen as an explicit example, where the action of $\hat{\mathcal{T}}^{\mathrm{ab}}_{\mathrm{id}}$ becomes equivalent to the permutation of coordinates

$$\hat{\mathcal{T}}^{\mathrm{ab}}_{\mathrm{id}} P_{2\mathrm{D},q}(\tau, h_1, h_2) = P_{2\mathrm{D},q}(\tau, h_2, h_1)\,. \tag{25}$$

Thus, the symmetry with respect to interchange of extra dimensions h_1, h_2 can be achieved through $P_{2\mathrm{D},q} + \hat{\mathcal{T}}^{\mathrm{ab}}_{\mathrm{id}} P_{2\mathrm{D},q}$. In a straightforward analogous manner one can get an antisymmetric combination $P_{2\mathrm{D},q} - \hat{\mathcal{T}}^{\mathrm{ab}}_{\mathrm{id}} P_{2\mathrm{D},q}$. For a certain instant of time we proposed illustration which is depicted in Fig.(1)(b).

At the end of this subsection, we consider the next even simple example, where mixed boundary conditions take place. Now let the 2-end-point string be allowed to pass to the 1-end-point string by means of the homotopy $P^{(1,2)}_{q_1,q_2}(\tau, h, \eta) = (1-\eta)P^{(1)}_{q_1}(\tau, h) + \eta P^{(2)}_{q_2}(\tau, h)$ driven by the parameter η which varies from 0 to 1. In fact, this model can be seen as a variant of the 2D brane with extra dimensions h and η.

A. Partial compactification

In the frame of the string theory, the compactification attempts to ensure compatibility of the universe based on the four observable dimensions with twenty-six dimensions found in the theoretical model systems. From the standpoint of the problems considered here, the compactification may be viewed as an act of the information reduction of the original signal data, which makes the transformed signal periodic. Of course, it is not very favorable to close strings by the complete periodization of real input signals. Partial closure would be more interesting. This uses pre-mapping

$$\tilde{p}(\tau) = \frac{1}{N_\mathrm{m}} \sum_{m=0}^{N_\mathrm{m}-1} p(\tau + l_\mathrm{s} m)\,, \tag{26}$$

where the input of any open string (see e.g. Eq.(3), Eq.(7)) is made up partially compact.

Thus, data from the interval $< \tau, \tau + l_\mathrm{s}(N_\mathrm{m} - 1) >$ are being pressed to occupy "little space" $h \in < 0, l_\mathrm{s} >$. We see that as N_m increases, the deviations of $\tilde{p}$ from the periodic

signal become less pronounced. The idea is illustrated in Fig.(1)(c),(d). We see that the states are losing their original form (a),(b) are starting to create ripples.

For example, one might consider the construction of the $(\tilde{D}+1)$-brane

$$f_q\left(\frac{p(\tau+h_0)-p(\tau)}{p(\tau+h_0)}\right)\prod_{j=1}^{\tilde{D}} f_q\left(\frac{\tilde{p}_j^{(\pm)}(\tau+h_j)-\tilde{p}_j^{(\pm)}(\tau)}{\tilde{p}_j^{(\pm)}(\tau+h_j)}\right) \tag{27}$$

maintained by combining $(\tilde{D}+1)$ 1-end-point strings, where partial compactification in $\tilde{D}$ extra dimensions is supposed. Of course, the construction introduces auxiliary variables $\tilde{p}_j^{(\pm)}(\tau)=\sum_{m=0}^{N_{\mathrm{m}},j-1} p(\tau \pm m\, l_{\mathrm{s},j})$.

6. STATISTICAL INVESTIGATION OF 2-END-POINT STRINGS

A. The midpoint information about string

In our present work, the strings and branes represent targets of physics-motivated maps which convert an originally dynamic range of currency data into the static frame. Of course, the data shaped by the string map have to be studied by the statistical methods. However, the question remains open about the selection of the most promising types of maps from the point of view of interpretation of their statistical response.

Many of the preliminary numerical experiments we performed indicating that the 2-end-point strings with a sufficiently high q (in this work we focus on $q=6$, but other unexplored values may also be of special interest) yield interesting statistical information including focus on rare events. Unfortunately, there is difficult or impossible to be exhaustive in this aspect. Figure(3) shows how $< P_6^{(2)}(\tau,h) >$ and the corresponding dispersion σ_{P_6} change with a string length.

B. The analysis of $P_q(l_{\mathrm{s}}/2)$ distributions

The complex trade fluctuation data can be characterized by their respective statistical moments. In the case of the string map the moments of the ξth order can be naturally considered at the half length

$$\mu_{q,\xi}=\left\langle\, |P_q^{(N_l)}(\tau,l_{\mathrm{s}}/2)|^{\xi/q}\right\rangle . \tag{28}$$

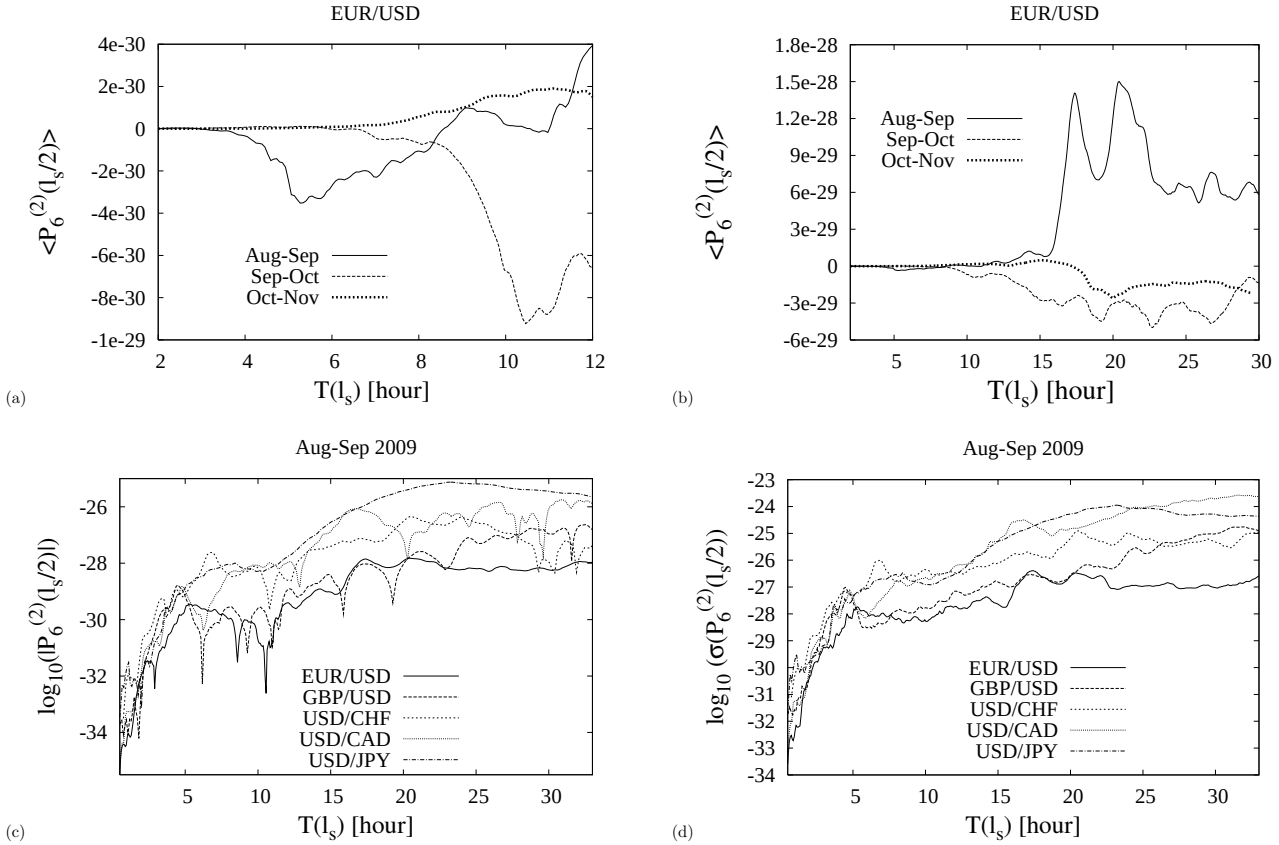

FIG. 3: The illustrative calculations carried out for EUR/USD currency. Figure shows the parts (a),(b) which include a view of two different epochs (and their different details). We see the variability of the mean statistical characteristics of the 2-end-point open string. The part (b) turns in sign, but remarkable exceptional scales corresponding to the local maxima and minima remain the same. The string length is expressed in real-time units calculated by means of Eq.(1). In part (c) we present anomalies - peaks roughly common for different currencies. These picture of anomalies are supplemented by dispersions of $P_q^{(2)}(l_{\rm s}/2)$ (d).

The comparison of the results obtained for the 1-end point and 2-end point strings is depicted in Fig.4. The remarkable difference in the amplitudes is caused by the manner of anchoring. The moments of longer strings are trivially larger.

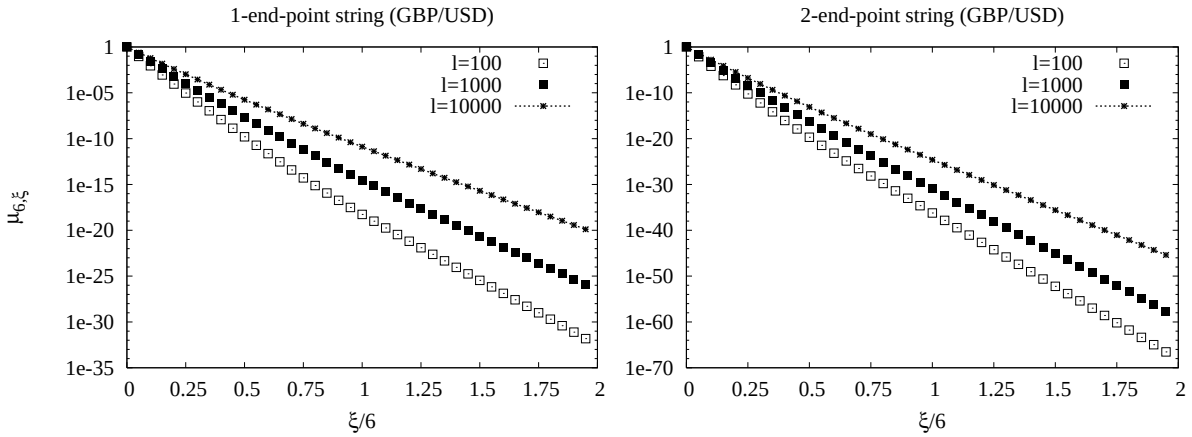

FIG. 4: The mid-point fluctuations characterized by the statistical moments defined by Eq.(28). The calculations are carried out for GBP/USD currency rate, for Aug-Sep period, for different kinds of strings for several lengths. We see that fluctuations become more significant as the string size increases. In addition, one may observe the 2-end-point string to be more suppressive to the fluctuations.

C. Volatility vs. string amplitude

The volatility as described here refers to the standard deviation of currency returns of a financial instrument within a specific time horizon described by the length $l_s/2$. The return volatility at the time scale $l_s/2$ is defined by $\sigma_r(l_s/2) = \sqrt{r_2(l_s/2) - r_1^2(l_s/2)}$ using $r_m(l_s) = \sum_{h=1}^{l_s/2}[(p(\tau+h) - p(\tau+h-1))/p(\tau+h)]^m$ for $m = 1, 2$. In Fig.(5), the *rate of return volatility* computed at the scale $L = l_s/2$ demonstrates the linkage to the changes in the price trend represented by $P_6^{(2)}(l_s/2)$. Since the trend changes do not follow Gaussian distributions, we have used high q to analyze the impact of rare events. In Fig.(5), we show the identification of the semi-discrete levels of volatility by $q = 6$, while setting $q = 1$ does not uncover common attributes.

7. INTRA-STRING STATISTICAL PICTURE

The idea of the string related maps proposed here is the transformation of the original point object such as selected single price into a system of a prices from its admissible neighborhood. This changeover from a local to a non-local description directly extends

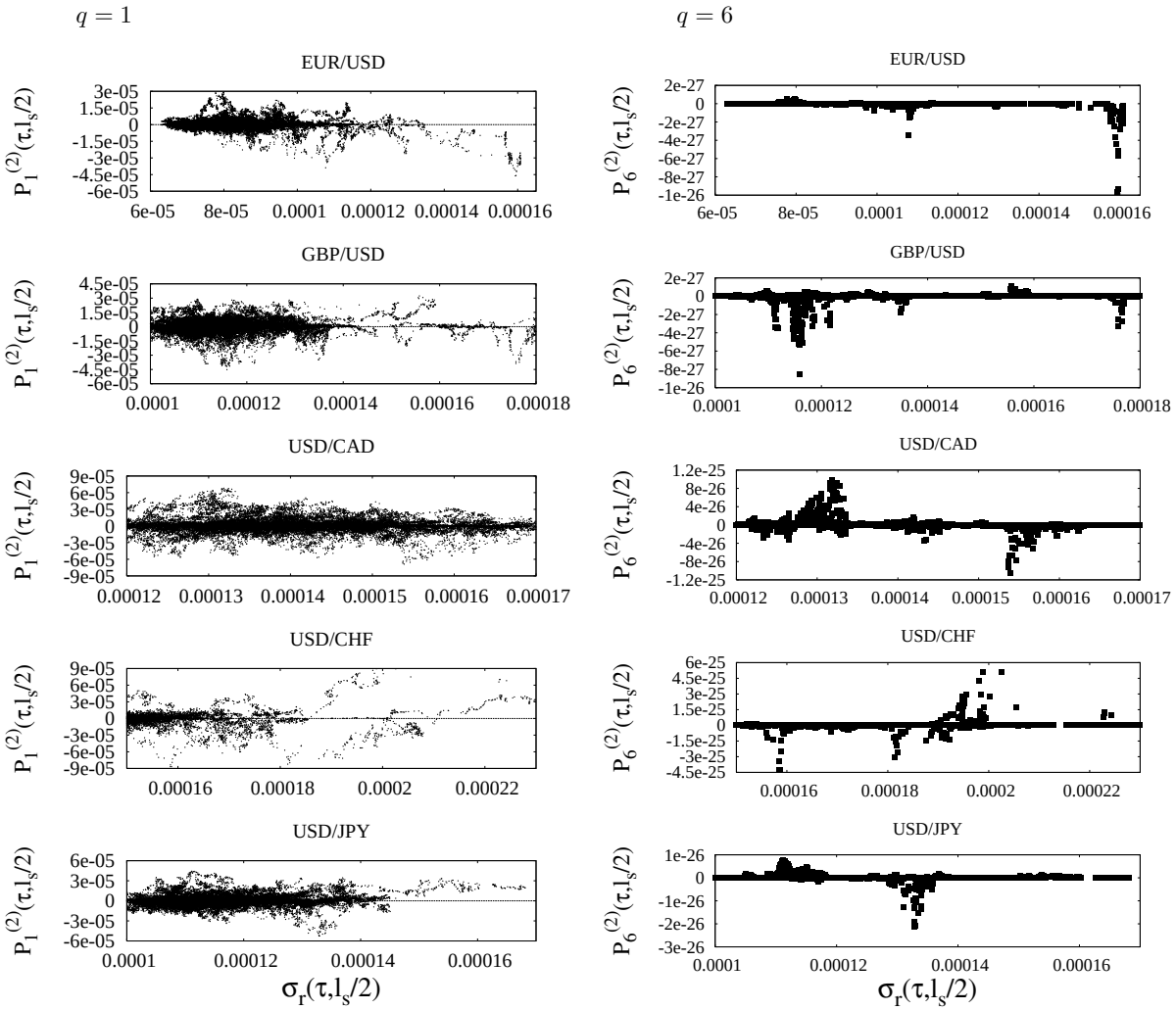

FIG. 5: The scatterplot showing the relationship between the volatility $\sigma_r(\tau, l_s/2)$ and the string amplitudes $P_1^{(2)}(l_s/2)$ ($q = 1$) and $P_6^{(2)}(l_s/2)$ ($q = 6$), respectively. The separating effect at high q is visible. The plot indicates conservation or brake of the price trend $P_6^{(2)}(l_s/2)$ over the tick time $< \tau, \tau + l_s >$. We see that the trend becomes coupled with the occurrence of specific isolated values of the volatility calculated for $l_s = 10000$; period Aug-Sep.

econometrics belief that future prices are deducible from the price history of a given period. The results of the investigation of the intra-string statistics for a selected scale l_s (period) are presented in Fig.(6).

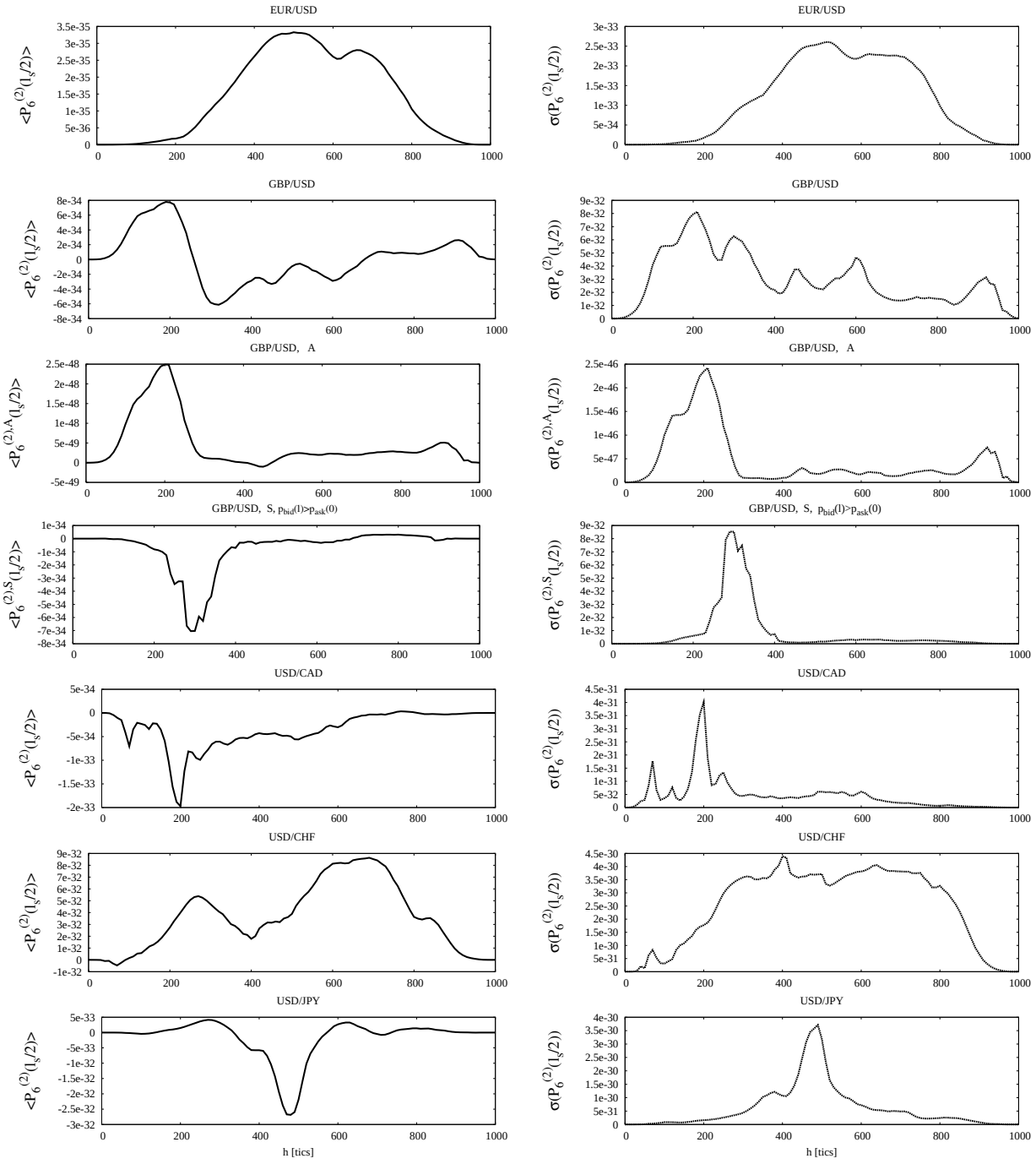

FIG. 6: The intra-string statistics for five currency pairs during the Aug-Sep period; the 2-end-point string is studied for $q = 6$, $l_{\rm s} = 1000$. The mean $< P_6^{(2)}(l_{\rm s}/2) >$ (l.h.s. column) and dispersion (r.h.s. column) of $P_6^{(2)}(\tau, h)$. The specific scope brings analysis of the effects of symmetry and spread for statistics collected within constraint that GBP/USD base currency is trending up ($p_{\rm bid}(l_{\rm s}) \geq p_{\rm ask}(0)$). The amplitude of $< P_6^{(2),{\rm A}}(l_{\rm s}/2) >$ is very small (fluctuations are suppressed) as compared to the average of the symmetric part. On the other hand, $< P_6^{(2),{\rm S}}(l_{\rm s}/2) >$ is not taken into plot since it is indistinguishable from $< P_6^{(2)}(l_{\rm s}/2) >$.

A. Time invariant strings and elementary statistics

To understand better the outputs of our numeric attempts, let us suppose to deal with short-time evolution of the currency $\ln p(\tau) = \ln p_0 + b\tau$ characterized by the linear-logarithmic parameter b. Surprisingly, after the substitution into the string, Eq.(7), the expressions collapse to the invariant (independent of τ) form

$$\begin{aligned} P_1^{(1)}(\tau, h) &= 1 - \exp(-hb)\,, \\ P_1^{(2)}(\tau, h) &= 1 - \exp[(h - l_{\rm s})b] - \exp(-hb) + \exp(-l_{\rm s}b)\,. \end{aligned} \tag{29}$$

It is quite interesting to look at the lowest order terms of Taylor series of this result around $b = 0$. Ignoring the terms of order b^4 or higher gives $P_1^{(1)} = bh - \frac{1}{2}b^2h^2 + \mathcal{O}(b^3)$, $P_1^{(2)} = b^2h(l_{\rm s} - h) + \mathcal{O}(b^3)$. It demonstrates that the model of the 1-end-point string is more sensitive to the sign of b variations.

The elementary qualitative statistical model of the string can be obtained by taking the unexamined assumption that b fluctuates with the Gaussian probability density $(2\pi\sigma_{\rm b}^2)^{-1}\exp[-b^2/(2\sigma_{\rm b}^2)]$. The averaging of Eq.(29) with this weight yields

$$< P_1^{(1)} >_{\rm Gauss}(h) = 1 - \exp\left(-\frac{h^2\sigma_{\rm b}^2}{2}\right)\,, \tag{30}$$

$$< P_1^{(2)} >_{\rm Gauss}(h) = 1 - \exp\left(-\frac{h^2\sigma_{\rm b}^2}{2}\right) - \exp\left(-\frac{(h - l_{\rm s})^2\sigma_{\rm b}^2}{2}\right) + \exp\left(-\frac{l_{\rm s}^2\sigma_{\rm b}^2}{2}\right)\,. \tag{31}$$

Equation(30) predicts an increase in the h dependence as a consequence of the symmetric fluctuations in b. This finding does not agree with the result presented in Fig.(2), where the mean string output is biased by the mean trend.

B. Mapping of the periodic input signal

Simultaneously with giving numerical results obtained for statistical averages of data, it is instructive to briefly examine the string map of the signal of periodic form described by some elementary function. The input signal $p(\tau) = a_1 + a_2\cos(\omega\tau)$ can be suitable for this purpose. Subsequently, the analytic calculation for the 2-end-point map can be carried out perturbatively under the requirement $a_2 \ll a_1$. The common form of average unifying formulas obtained for different integer q values can be written as

$$< P_q^{(2),({\rm S})}(h) >_{\cos} = [\cos(h\omega) + \cos((h - l_{\rm s})\omega) - \cos(l_{\rm s}\omega) - 1]^q \sum_{j=0} c_{q,j}\left(\frac{a_2}{a_1}\right)^{2(q+j)}\,, \tag{32}$$

where $c_{q,j}$ are the numerical coefficients which are not critical for further reasoning. The intuitive idea that $P_q^{(2),(\mathrm{A})}(\tau,h)$ discriminates fluctuations, which stems from the comparison of the symmetric and antisymmetric averages (see Fig.(6)), is partially justified by the result $< P_q^{(2),(\mathrm{A})}(h) >_{\cos} = 0$.

Interestingly, the calculation highlights the idea of the presence of the resonant lengths $l_{\mathrm{s}}(n) = 2\pi n/\omega$ as $n = 1, 2, \ldots$. This basic result motivated us to introduce the 2-end-point string model, that has potential to identify characteristic dynamic scales represented here by $1/\omega$. It is important that anomalous aspect is absent in the statistical characteristics of the one-point strings.

C. String map in the representation of internal Fourier modes

At each tick τ the string may be represented by the sequence $P_q^{(2)}(\tau,h)$, $h = 0, 1, \ldots, l_{\mathrm{s}}-1$ which can be transformed by means of the discrete Fourier transform

$$P_{\mathrm{DFT},q}(k,\tau) = \sum_{h=0}^{l_{\mathrm{s}}} P_q^{(2)}(\tau,h) \exp\left(-\frac{2\pi i k h}{l_{\mathrm{s}}+1}\right), \quad k = 0, 1, \ldots, l_{\mathrm{s}}\,. \tag{33}$$

Having done this, one can introduce the inverse transform

$$P_{\mathrm{IDFT},q}(h,\tau) = \sum_{k=0}^{l_{\mathrm{s}}} P_{\mathrm{DFT},q}(\tau,k) \exp\left(\frac{2\pi i k h}{l_{\mathrm{s}}+1}\right), \tag{34}$$

which can be understood as a periodic extension of the input $P_q^{(2)}(\tau,h)$ with a period of the $(l_{\mathrm{s}}+1)$ ticks. Then $P_{\mathrm{IDFT},q}(h,\tau)$ can be viewed as a portion of the original signal which curls up along the *compact dimension* of the *closed string*. Thus, the integer $h/(l_{\mathrm{s}}+1)$ has the meaning of a winding number of $P_{\mathrm{IDFT},q}(h,\tau)$. The statistical mean values of $P_{\mathrm{DFT},q}(k,\tau)$ calculated for different currencies are depicted in Fig.(7). The Fourier transform of the inherent string structure may serve to identify distinguishing features of currencies at selected time scale.

8. STRING POLARIZED BY THE EXTERNAL FIELD

In this section, we modify the two-point-string model, Eq.(7), in order to account for the transaction costs. A natural way is to consider the relation for the spread-adjusted return

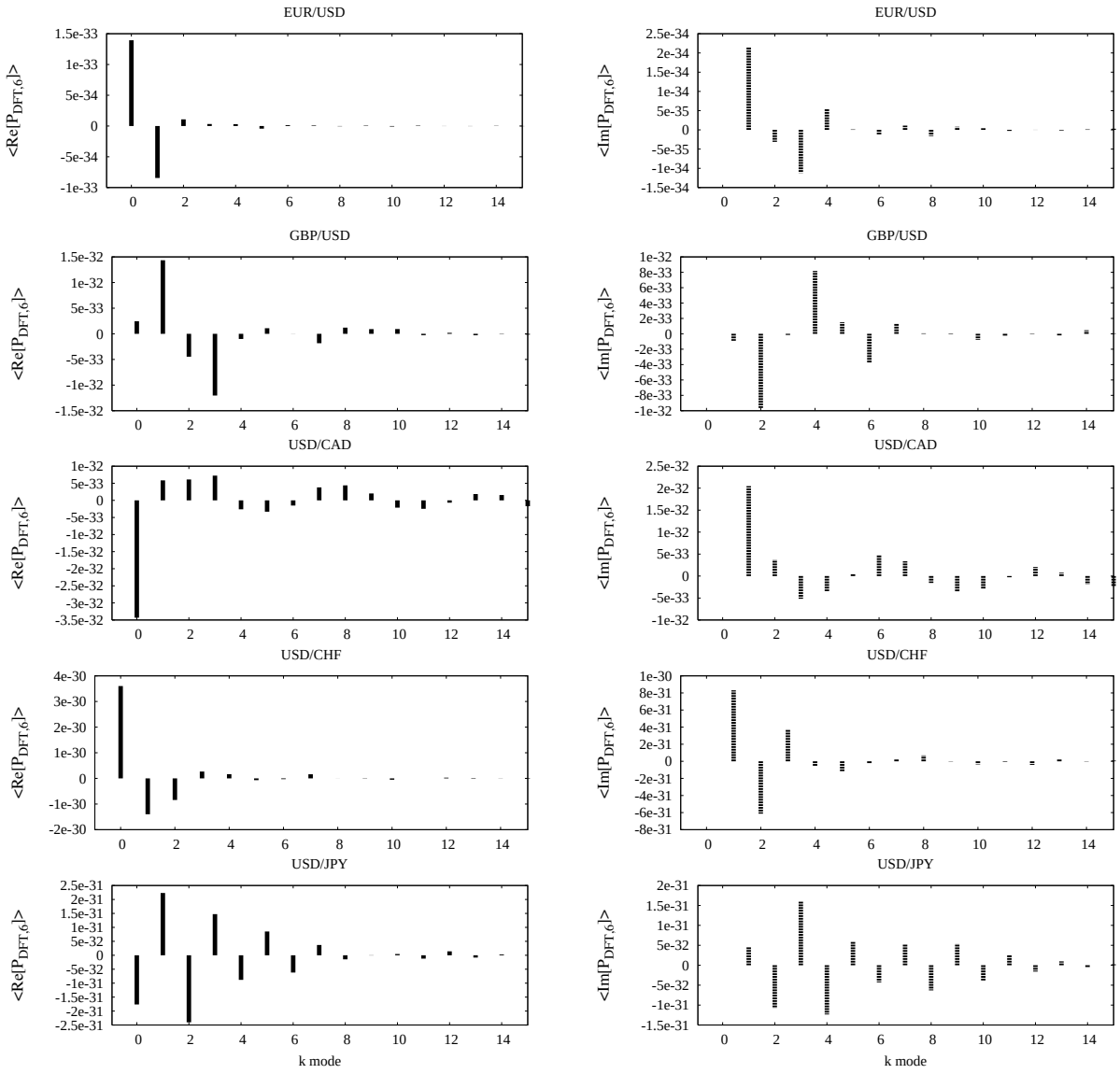

FIG. 7: The currency-specific slow ($k \leq 14$) intra-string averaged Fourier modes (their real and imaginary part separately) obtained by the temporal averaging over the Aug-Sep period. The mean real and imaginary parts calculated for five pairs, $q = 6$ and string length $l_{\rm s} = 1000$.

$(p_{\rm bid}(\tau+h) - p_{\rm ask}(\tau))/p(\tau+h)$ (written here for a long position). If we now routinely extend the 2-end-point, Eq.(7), we obtain

$$P_q^{\rm ab}(\tau, h) = f_q \left(\left(\frac{p_{\rm bid}(\tau+h) - p_{\rm ask}(\tau)}{p(\tau+h)} \right) \left(\frac{p_{\rm bid}(\tau+l_{\rm s}) - p_{\rm ask}(\tau+h)}{p(\tau+l_{\rm s})} \right) \right) . \qquad (35)$$

However this clearly violates, the Dirichlet boundary conditions, Eq.(8). The spread itself yields a negligible correction to the mean values.

The boundary conditions can be easily renewed by the subtraction $\tilde{P}_q^{\rm ab}(\tau,h)=P_q^{\rm ab}(\tau,h)-P_q^{\rm ab}(\tau,0)$. However, we show there exists a more fundamental alternative way which reflects a bid-ask difference and preserves the Dirichlet boundary conditions. The string states are *polarized* by the instant possibility to place a successful/unsuccessful buy order. For each h and $Y=A,S$ we construct the inequality constrained sequence

$$P_{(q,+)}^{(2),Y}(\tau+1,h)=\begin{cases} P_q^{(2),Y}(\tau,h)\,,\ p_{\rm bid}(\tau+l_{\rm s})\geq p_{\rm ask}(\tau) \\ P_{(q,+)}^{(2),Y}(\tau,h)\,,\ \text{otherwise} \end{cases} \tag{36}$$

and non-buy contributions, respectively,

$$P_{(q,-)}^{(2),Y}(\tau+1,h)=\begin{cases} P_q^{(2),Y}(\tau,h)\,,\ p_{\rm bid}(\tau+l_{\rm s})< p_{\rm ask}(\tau) \\ P_{(q,-)}^{(2),Y}(\tau,h)\,,\ \text{otherwise}\,. \end{cases} \tag{37}$$

In both cases it is supposed that $P_q^{(2),Y}(\tau,h)$ is calculated according an unconditioned model defined by Eq.(7). Now, to characterize the arbitrage opportunities, we introduced the statistical polarization measure in the form

$$g_{q,Y}=\Big\langle\frac{\sum_{h=0}^{l_{\rm s}}|P_{(q,+)}^{(2),Y}(\tau,h)-P_{(q,-)}^{(2),Y}(\tau,h)|}{\sum_{h=0}^{l_{\rm s}}|P_{(q,+)}^{(2),Y}(\tau,h)+P_{(q,-)}^{(2),Y}(\tau,h)|}\Big\rangle\,,\quad Y=A,S\ . \tag{38}$$

The results of the extensive study of this measure are depicted in Fig.8.

We continue the characterization of arbitrage opportunities by defining the(momentum) distance function between the strings as

$$d_q^{(Y)}(\tau)=\frac{1}{l_{\rm s}+1}\sum_{h=0}^{l_{\rm s}}\Big|\,P_{(q,+)}^{(Y)}(\tau,h)-P_{(q,-)}^{(Y)}(\tau,h)\Big|\ . \tag{39}$$

In this case the statistics of string distances can be characterized by the customized variant of the well-known model of the *correlation sum* [7, 13, 14]. However, the motivation here differs from that given in these papers, where the intent was to analyze nonlinear relationships. The correlation sum shows the probability that the states of two strings or branes are localized within a certain distance. In our view we adjust the original formula to the string and brane models which, in addition, reflect the transactions involving profits. We define the measure

$$C_q^{(Y)}(\epsilon)=\frac{\langle\Theta(\epsilon-d_q^{(Y)}(\tau))\rangle}{\int{\rm d}\epsilon'\,\langle\Theta(\epsilon'-d_q^{(Y)}(\tau))\rangle}\,, \tag{40}$$

where ϵ is the threshold distance, $\Theta(.)$ is the Heaviside step function; here $l_{\rm s}$ plays the role of so called embedding dimension. The key concept surrounding this measure is the concept of

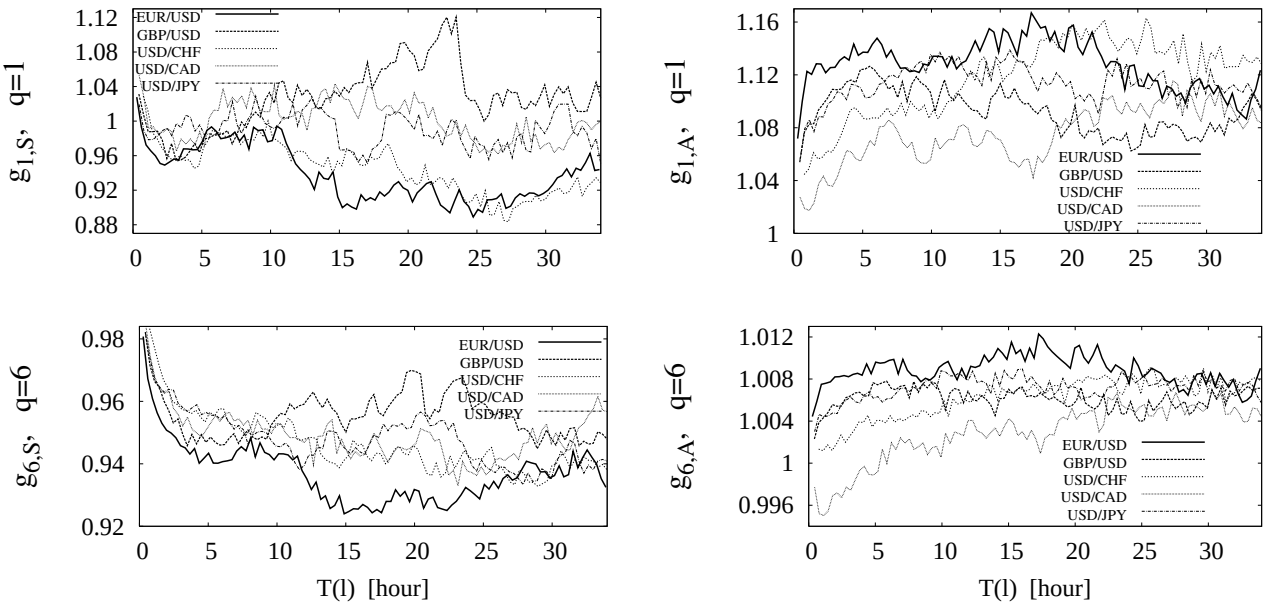

FIG. 8: The effect of string polarization on the mean characteristics calculated for selected currency pairs. One might identify a sudden increase of intra-string distinguishing features for the scales ranging from to 3-5 hours.

the fractal dimension. In Fig.(9) we estimated a specific fractal dimension $D_{\rm F}$ as a slope of the dependence $\mathrm{d}\ln C_q^{(Y)}(\epsilon) = D_{\rm F}\mathrm{d}\ln\epsilon$. However, as the figure shows, we have extended our construction further and extend the concept of distance for 2D branes as defined in Eq.(23). In a case like this we suggest generalization

$$d_{2\mathrm{D},q}(\tau) = \frac{1}{(l_{\rm s}+1)^2}\sum_{h_1=0}^{l_{\rm s}}\sum_{h_2=0}^{l_{\rm s}}\left|P_{2\mathrm{D},(q,+)}(\tau,h_1,h_2) - P_{2\mathrm{D},(q,-)}(\tau,h_1,h_2)\right| . \qquad (41)$$

9. INTER-CURRENCY STUDY: MAP ONTO ROTATING STRINGS

The incorporating of the mutual relations between the pairs into the mapping procedure represents a very challenging task. Let us study trading activity in the (I, J) plane, where I, J stands for indices of the currency pair described by two 2-end-point strings. The real time data are used instead of tick by tick (see sec.2) in order to maintain the consistency of prices quoted.

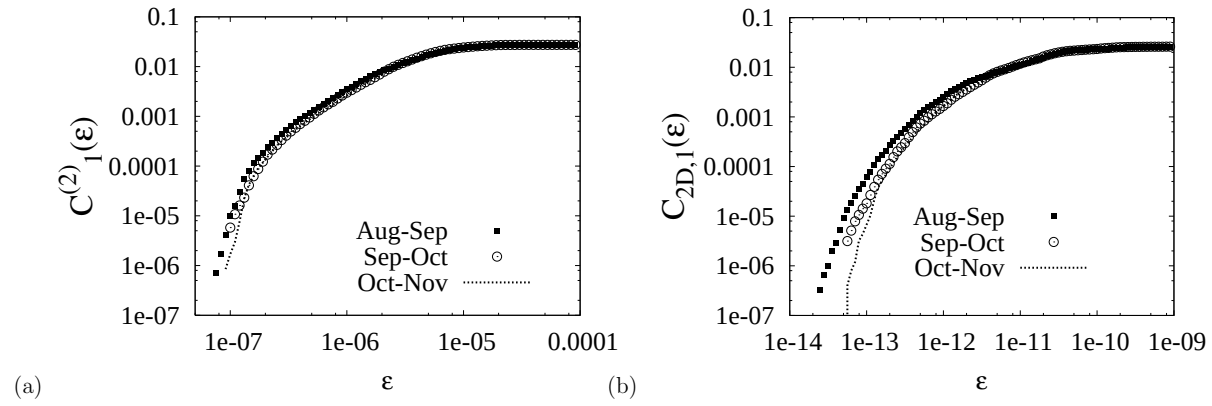

FIG. 9: The figure showing the statistics of inter-string distances. In part (a) the statistics collected and organized for the 2-end-point strings by means of the correlation sum (see Eq.(39)) for the currency pair GBP/USD and three time periods. As expected, the function $C_q^{(Y)}(\epsilon)$ monotonically decreases to zero as $\epsilon \to 0$. The index $D_{\rm F} = 1.25 - 1.26$ varies over the periods. The values have been obtained by fitting over the estimated *universality range* $< 10^{-7}, 2.10^{-6} >$ of ϵ. In part (b) the exponential dependences $C_{2{\rm D},1}(\epsilon)$ are obtained after the replacement of $d_q^{(Y)}(\tau)$ by $d_{2{\rm D},q}(\tau)$ in Eq.(40). We see that the inter-brane distances follow the exponential-type law with the highest variability across the short distances.

By continuing examples of the generalized distance concept (see Eq.(39)) and Eq.(41), we can introduce the inter-currency momentum distance function

$$d_{q,I,J}(t) \;=\; \frac{1}{l_{\rm s}+1}\sum_{h=0}^{l_{\rm s}} \left| P_{q,I}^{(2)}(t,h) - P_{q,J}^{(2)}(t,h) \right|. \tag{42}$$

At higher dimension, it is tempting to deal with angular momentum

$$M_{q,I,J}(t) = \sum_{h=0}^{l_{\rm s}} \left[P_{q,I}^{(2)}(t,h) X_{q,J}^{(2)}(t,h) - P_{q,J}^{(2)}(t,h) X_{q,I}^{(2)}(t,h) \right]. \tag{43}$$

The momentum calculation can be interpreted as a measure of the rotational information flows between the currency pairs. In Fig.(10) we present the results achieved for two alternatives $(I,J) = ({\rm EUR/USD}, {\rm GBP/USD})$, and $(I,J) = ({\rm GBP/USD}, {\rm USD/JPY})$. We see that calculation of $D_{q,I,J}$ and $M_{q,I,J}$ yields oscillatory (i.e. seasonal) behavior. Simultaneously, the concept of distance and moment has been extended to analyze the impact of spread. Analogously, as in the previous cases, the distance between the ask and bid strings may be

defined

$$d^{\rm ab}_{q,I}(t) \;=\; \frac{1}{l_{\rm s}+1}\sum_{h=0}^{l}\Big|P^{(2)}_{q,{\rm ask}}(t,h)-P^{(2)}_{q,{\rm bid}}(t,h)\Big|\,, \tag{44}$$

$$M^{\rm ab}_{q,I}(t) \;=\; \sum_{h=0}^{l_{\rm s}}\Big[\,P^{(2)}_{q,{\rm ask}}(t,h)X^{(2)}_{q,{\rm bid}}(t,h)-P^{(2)}_{q,{\rm bid}}(t,h)X^{(2)}_{q,{\rm ask}}(t,h)\Big]\,. \tag{45}$$

Here

$$P^{(2)}_{q,{\rm ask}}\equiv P^{(2)}_{q}|_{p\to p_{\rm ask}}\,,\quad P^{(2)}_{q,{\rm bid}}\equiv P^{(2)}_{q}|_{p\to p_{\rm bid}} \tag{46}$$

are obtained by substituting expressions above in Eq.(7). With the help of Eq.(9) and $P^{(2)}_{q,{\rm ask}}$, $P^{(2)}_{q,{\rm bid}}$ we construct iteratively $X^{(2)}_{q,{\rm ask}}$ and $X^{(2)}_{q,{\rm bid}}$. As one can see from Fig.(10), the differences measured in terms of $M_{q,I,J}(t)$ are very subtle. There is evidence of intercoupling of the spread and currency dynamics. The fundamental role in the string theory is played by the *Regge slope parameter* α' (or inverse string tension). This has a proper analogy with our approach where we introduced a slope in terms of the angular momentum

$$\alpha'_{q,I,J}=\frac{<|M_{q,I,J}|>}{2\pi\, l_{\rm s}^2}\,. \tag{47}$$

For the $l_{\rm s}=1$hour string pair we obtained $\alpha'_{6,{\rm EUR/USD,\ GBP/USD}}=5.07.10^{-54}\ (2\pi)^{-1}\ {\rm hour}^{-2}$, $\alpha'_{6,{\rm GBP/USD,\ USD/JPY}}=1.55.10^{-53}\ (2\pi)^{-1}\ {\rm hour}^{-2}$, $\alpha'_{6,{\rm USD/JPY,\ EUR/USD}}=1.34.10^{-53}\ (2\pi)^{-1}\ {\rm hour}^{-2}$ much larger than the spread $\alpha^{\rm ab}_{6,{\rm GBP/USD}}=1.16\cdot 10^{-55}\,(2\pi)^{-1}{\rm hour}^{-2}$. However, it is worth noting that relation, Eq.(47), should be understood as an estimate since there is no statistical mean of the type $<|M_{...}|>$ in the original specification. The problem of estimation of the *slope parameter* arises from the fact that in the original model nonaveraged angular momentum is divided by the square of the mass instead of $l_{\rm s}^2$. Herein, we have no idea how to measure the mass of the string, or how to verify the fact that the string mass is proportional to $l_{\rm s}$.

10. DIFFERENTIALS OF STRING MAP

Gâteaux derivative is a generalization of the concept of a directional derivative in the differential calculus. In our study the concept can be viewed as a systematic way in the generation of more structured maps expressing more information about the structure of

data we deal with. Given the string map $P(.)$, the m-th *Gâteaux derivative* of $P(.)$ in the "direction" of $\psi(.)$ (unspecified yet series) is defined as follows:

$$\mathrm{d}^m P(\{p\};\{\psi\})(\tau,h) = \frac{\mathrm{d}^m}{\mathrm{d}\epsilon^m} P(\{p(\tau,h)+\epsilon\psi(\tau,h)\})\Big|_{\epsilon\to 0}\,. \tag{48}$$

For $q=1$ the calculation gives

$$\mathrm{d}P_1^{(1)}(\{p\};\{\psi\})(\tau,h) = \frac{1}{p(\tau+h)}\left[\frac{p(\tau)\psi(\tau+h)}{p(\tau+h)} - \psi(t)\right] \tag{49}$$

and

$$\mathrm{d}P_1^{(2)}(\{p\};\{\psi\})(\tau,h) = \psi(\tau)\left(\frac{1}{p(\tau+l_{\mathrm{s}})} - \frac{1}{p(\tau+h)}\right) \tag{50}$$
$$+\ \psi(\tau+h)\left(\frac{p(\tau)}{p^2(\tau+h)} - \frac{1}{p(\tau+l_{\mathrm{s}})}\right) + \frac{\psi(\tau+l_{\mathrm{s}})}{p^2(\tau+l_{\mathrm{s}})}\left(p(\tau+h)-p(\tau)\right)\,.$$

By going to the second order we obtained

$$\mathrm{d}^2 P_1^{(2)}(\{p\};\{\psi\})(\tau,h) = \frac{2\psi(\tau+h)}{p^2(\tau+h)}\left[\psi(\tau) - \frac{p(\tau)\psi(\tau+h)}{p(\tau+h)}\right] \tag{51}$$

and

$$\mathrm{d}^2 P_1^{(2)}(\{p\};\{\psi\})(\tau,h) = \frac{2\psi(\tau+l_{\mathrm{s}})}{p^2(\tau+l_{\mathrm{s}})}\left[\psi(\tau+h)-\psi(\tau)\right] \tag{52}$$
$$+\ \frac{2\psi(\tau+h)}{p^2(\tau+h)}\left[\psi(\tau) - \frac{p(\tau)\psi(\tau+h)}{p(\tau+h)}\right] + \frac{2\psi^2(\tau+l_{\mathrm{s}})}{p^3(\tau+l_{\mathrm{s}})}\left[p(\tau)-p(\tau+h)\right]\,.$$

Surprisingly, the generalized differentiation generates maps which satisfy the Dirichlet boundary conditions

$$\mathrm{d}^m P_1^{(1)}(\{p\};\{\psi\})(\tau,0) = 0\,, \qquad m=1,2; \tag{53}$$

$$\mathrm{d}^m P_1^{(2)}(\{p\};\{\psi\})(\tau,0) = \mathrm{d}^m P_1^{(2)}(\{p\};\{\psi\})(\tau,l_{\mathrm{s}}) = 0\,. \tag{54}$$

Many alternative ways exist to exploit the models with the auxiliary field $\psi(.)$. The field can be related to, e.g., (i) models which place emphasis on the currency margins determined by some adaption process; (ii) on the spread in a style of sec.8 with $\psi(\tau) = p_{\mathrm{bid}}(\tau) - p_{\mathrm{ask}}(\tau - l_{\mathrm{s}})$. (iii) The benchmark setting represents $\psi = 1$, (iv) the periodic function $\psi(\tau)$ can model the action of the compact. In this intuition supporting case, one can see that the generalized derivative modifies the original map as follows:

$$\mathrm{d}P_1^{(1)}(\{p\};\{\psi\})(\tau,h)|_{\psi=1} \;=\; -\frac{P_1^{(1)}(\tau,h)}{p(\tau+h)}\,, \tag{55}$$

$$\mathrm{d}P_1^{(2)}(\{p\};\{\psi\})(\tau,h)|_{\psi=1} \;=\; \left(\frac{1}{p(\tau+h)} + \frac{1}{p(\tau+l_{\mathrm{s}})}\right) P_1^{(2)}(\tau,h)\,. \tag{56}$$

In Fig.10, we present the idea, where p, ψ are represented by two currencies, their mutual influence is studied within the first-order differential model described by Eq.(50).

11. CONCLUSIONS

We shown that the string theory may motivate the adoption of the nonlinear techniques of the data analysis with a minimum impact of justification parameters. The numerical study recovered interesting fundamental statistical properties of the maps from the data onto string-like objects. The remarkable deviations from the features known under the notion of the efficiently organized market have been observed, namely, for high values of the deformation parameter q.

The main point here is that the string map gives a geometric interpretation of the information value of the data. The model of the string allows one to manipulate with the information stored along several extra dimensions. We started from the theory of the 1-end-point and 2-end-point string, where we distinguished between the symmetric and antisymmetric variants of the maps. In this context, it should be emphasized that duality is a peculiar property of the suggested maps, not data alone. The numerical analysis of the intra-string statistics was supplied qualitatively by the toy models of the maps of the exponential and periodic data inputs. Most of the numerical investigations have been obtained for the open topology; however, we described briefly the ways to partial compactification. The data structures can also be mapped by means of the curled dimension which arises as a sum of periodic data contributions. The idea of the compactified strings can be realized as well by the application of the inverse Fourier transform of the original signal. The interesting and also challenging task represents finding of link between string map and log-periodic behaviour of speculative bubbles of the stock market indices [15, 16]. It would be also interesting to examine R/S analysis of the Hurst exponents [17, 18] for the case of finite strings instead of the usual point prices.

The study of string averages exhibited occurrences of the anomalies at the time scales proportional to the string length. We showed that global and common market timescales can be extracted by looking at the changes in the currencies. The extensions of the string models of branes including ask/bid spread were discussed. We studied the relationship between the arbitrage opportunities and string statistics. We showed that extraction of the

valuable information about the arbitrage opportunities on given currency could be studied by means of the correlation sum which reflected the details of the occupancy of phase-space by differently polarized strings and branes. In addition, we presented several physics and geometry motivated methods of analysis of the coupling between the currency pairs. The results led us to believe that our ideas and methodology can contribute to the solution of the problem of the robust portfolio selection. As we have seen, the complex multi-string structures produced by the generalized derivatives of strings cannot be easily grasped by the intuitive principles. We believe, the method affords potential to be used in the practical applications, where arbitrage selection bias should be taken into account.

---

[1] D.McMahon, "String theory demystified", The McGraw-Hill Companies, Inc., (2009).

[2] B.Zwiebach, "A first course in string theory", Cambridge university press, (2009).

[3] J.He and M.Deem, PRL 198701, 188 (2010).

[4] W.S.Jung, O.Kwon, F.Wang, T.Kaizoji, H.T.Moon and H.E.Stanley, Physica A 387, 537 (2008).

[5] M.Eryiğit and R.Eryiğit, Physica A 388, 3551 (2009).

[6] P.R.Krishnaiah and L.Kanal, "Classification, Patterm Recognition, and Reduction of Dimensionality", North-Holland, Amsterdam (1982).

[7] P.Grassberger and I.Procaccia, Physica D 9, 189 (1983).

[8] Y.Ding, X.Yang, A.J.Kavs and J.Li, Int. J. of Trade, Economics and Finance 1, 320 (2010).

[9] Joseph Polchinski, "String Theory", Cambridge University Press, (1998).

[10] M.B.Green, J.H.Schwarz and E.Witten, "Superstring theory",Cambridge University Press, (1987).

[11] W.H.Wagner and M.Edwards, Finantial Analytists Journal 49, 65 (1993).

[12] R.Roll, The journal of finance 39, 1127 (1984).

[13] J.Y.Campbell, A.W.Lo and A.C.MacKinlay, "The Econometrics of Financial Markets", Princeton University press (1997).

[14] N.Bigdeli and K.Afshar, Physica A 388, 1577 (2009).

[15] W.X.Zhou and D.Sornette, Physica A 330, 543 (2003).

[16] W.X.Zhou and D.Sornette, Physica A 337, 243 (2004).

[17] B. Mandelbrot, Review of Economics and Statistics 53, 225 (1971).

[18] M.A.S. Granero, J.E.T. Segovia and J.G. Pérez, Physica A 387, 5543 (2008).

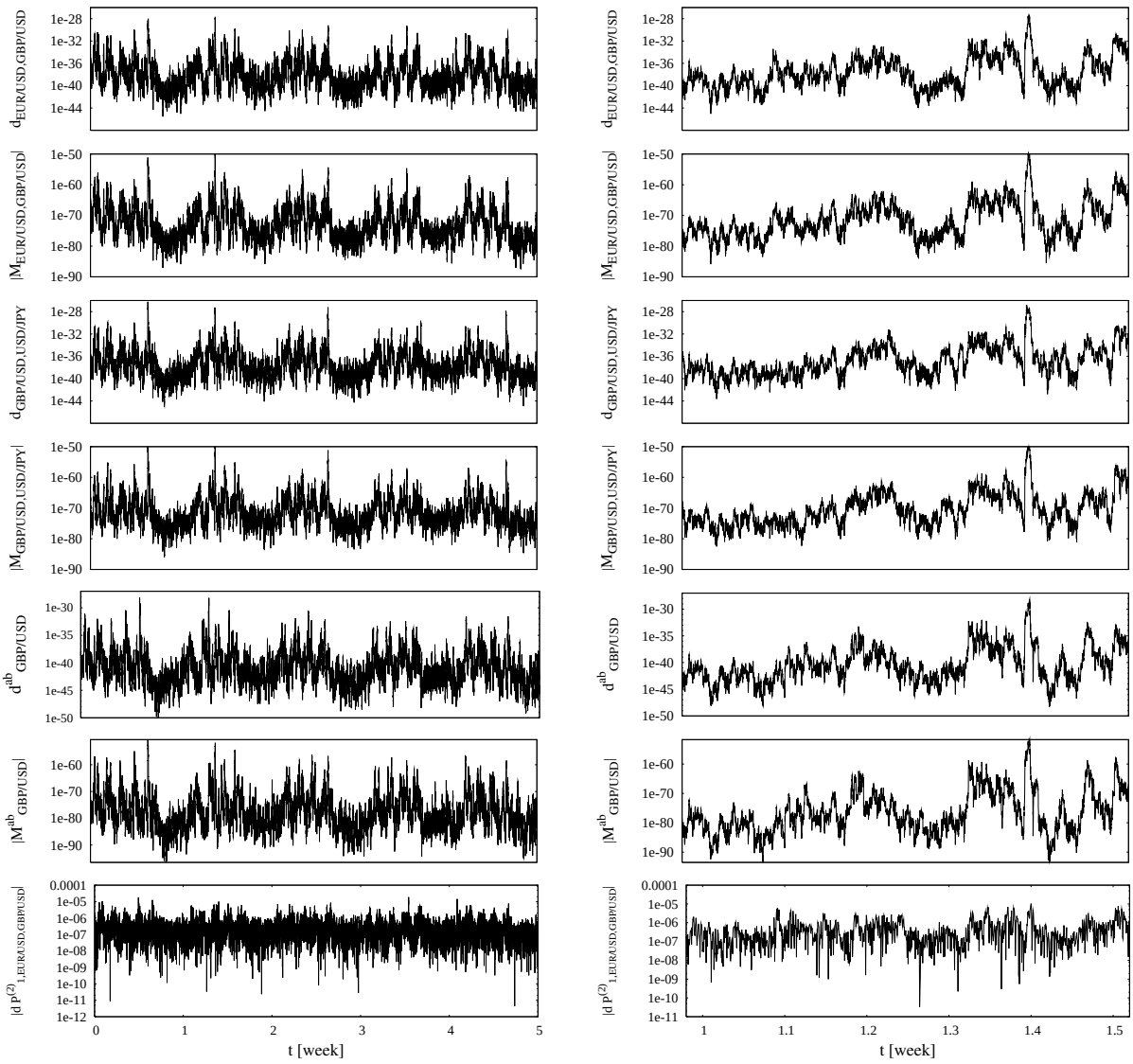

FIG. 10: The inter-string distance and angular momentum (see Eqs.(42) and (43)) for specified currency pairs. The long term outlook compared with a detailed one-week view supplemented by the results obtained for spread according to Eq.(44) and Eq.(45). The results are compared with the Gâteaux derivative (see Eq.(50), where p corresponds to EUR/USD and ψ to GBP/USD pair), and the derivative is evaluated at $h = l_{\rm s}/2$. The calculation is carried for the string of the 1-hour time length and investigation of the Aug-Sep period.